Local probing of magnetoelectric coupling and magnetoelastic control of switching in $BiFeO_3$-$CoFe_2O_4$ thin-film nanocomposite

Feng Yan,[1,2] Guannan Chen,[1] Li Lu,[2] Peter Finkel,[3] and Jonathan E. Spanier[1,a)]
[1]*Department of Materials Science & Engineering, Drexel University, Philadelphia, Pennsylvania 19104, USA*
[2]*Department of Mechanical Engineering, National University of Singapore, Singapore 117576*
[3]*US Naval Undersea Warfare Center, Code 1512, Newport, Rhode Island 02841, USA*

(Received 13 August 2012; accepted 12 July 2013; published online 25 July 2013)

We report on the combination of piezoresponse force microscopy (PFM), magnetic force microscopy, and local ferroelectric switching with magnetic field for the study of a thin-film magnetoelectric (ME) nanocomposite. The collection of PFM under an applied variable magnetic field within a polycrystalline perovskite-spinel $BiFeO_3$-$CoFe_2O_4$ (BFO-CFO) 0-3 type thin-film nanocomposite enables quantitative and proximal measurement of magnetoelastic strain-driven ME response. Combination of measurement of the as-grown strain state with local measurements of microstructure and macroscopic magnetization permits local mapping of ME coupling. © *2013 AIP Publishing LLC*. [http://dx.doi.org/10.1063/1.4816793]

Controlling coupling among electric polarization, strain, and magnetization in magnetoelectric (ME) materials is essential to realizing practical oxide based functional devices.[1,2] In ME multiferroics, coexistence of ferroelectric (FE) and ferromagnetic (FM) orderings permit coupling either directly between the two order parameters (intrinsic) or indirectly via strain (extrinsic).[3] $BiFeO_3$ (BFO) is among the most widely studied intrinsic room-temperature ME materials. Since it possesses strong FE polarization, but it is antiferromagnetic,[4] the design of extrinsic ME multiferroics has emerged as a promising and high-performance alternative to intrinsic multiferroics. Among two-component arrangements of constituent FE and FM phases are the particulate composite in which one phase is continuous (0–3), horizontal multilayers (2–2 connectivity scheme), and vertical heterostructures (1–3 connectivity).[5–7] Specifically, these designations refer to the following: the (0–3) scheme denotes a two-component arrangement of constituent FE and FM phases, where one phase is a continuous matrix and the other exists as inclusions embedded within the matrix phase; the (2–2) scheme involves a horizontal multilayer structure where the two constituents are parallel to each other; and the (1–3) scheme involves vertical heterostructures, where one component is in the form of a fiber-like structure embedded in a vertically aligned arrangement within the matrix of the other phase.

A number of candidate extrinsic multiferroics (materials combinations and material arrangements) have been investigated for enhancing the magnetization while retaining high electromechanical coupling from large ferroelectric polarizations. Among these are self-assembled columnar composites ($BaTiO_3$-$CoFe_2O_4$, $BiFeO_3$-$CoFe_2O_4$, $BaTiO_3$-$NiFe_2O_4$, or $PbTiO_3$-$CoFe_2O_4$),[8–10] well-ordered multiferroics[11] ($Pb(Zr,Ti)O_3$-$CoFe_2O_4$), and core-shell nanofibers[12] ($Pb(Zr,Ti)O_3$-$CoFe_2O_4$). Among $BiFeO_3$-$CoFe_2O_4$ (BFO-CFO) nanocomposites, lattice misorientation of the constituent materials plays a decisive role in determining the electronic and magnetic coupling at the oxide interface[7,13] with reports of controlling crystallographic orientations and magnetic properties via substrate selection.[13–15] Since the ME response of these nanocomposites is strain-tunable at the phase boundaries, control of the interface strain state through tailoring nanostructure geometry is essential.[16] Efforts to enhance the ME response in BFO-CFO have focused on epitaxial (1–3) and (2–2) nanostructures, including tuning the proportion of the ferrite phase.[17–19] However, reports on the ME response in polycrystalline BFO-CFO nanocomposites (approximately (0–3) schemes) are scant, despite expectations that a high ME response is predicted because of difficulties in preparation and leakage.[7]

Here we report on the local probing of the magneto-electromechanical coupling within a thin-film ME nanocomposite, specifically a polycrystalline BFO-CFO nanocomposite film. The composition (35% BFO to 65% CFO) was selected because the BFO response for this concentration has been reported to be the highest.[20] Specifically, it is easier to control the magnetoelastic effect in CFO with this composition (e.g., rather than 65% BFO and 35% CFO) and, further, to tailor the strain state in BFO via magnetoelastic coupling in CFO. To determine the ME response and to extract the local ME coupling within this nanocomposite with high spatial resolution, we use scanning probe microscopy (SPM) with a static and controllable magnetic field ($-2\,\text{kOe} < H < +2\,\text{kOe}$) applied within the plane of the thin-film nanocomposite. The FM magnetic domain variation and local control of FE switching are recorded under the same experimental conditions to quantify the ME response.

BFO-CFO nanocomposite thin films (thickness ~150 nm) were deposited on $Pt/TiO_2/SiO_2/Si(100)$ substrates via pulsed laser deposition (248 nm KrF excimer laser, 5 Hz repetition rate) using a $(BiFeO_3)_{0.35}$-$(CoFe_2O_4)_{0.65}$ target. The thin film product phase structures were determined using X-ray diffraction (XRD) with Cu $K\alpha$ radiation (Shimadzu XRD-7000). The Raman spectra were collected using a 514.5 nm Ar-ion laser as excitation at room temperature (Renishaw inVia). Macroscopic magnetic hysteresis loops were characterized with a vibrating sample magnetometer (VSM, Lakeshore 7400). The topographic height image of the nanocomposite surface was collected and its FE component properties were

a)Electronic address: spanier@drexel.edu

analyzed using piezoresponse force microscopy (PFM, Asylum Research MFP-3D) using an Ir/Pt-coated cantilever (Olympus AC240TM). To investigate ME coupling within the nanocomposite we used a variable field module (VFM, Asylum Research) to apply an in-plane variable magnetic field ($0 < H < 2$ kOe) during PFM characterization in order to image the evolution of ferroelectric domain structure and switching behavior induced by the external magnetic field. Here, PFM was implemented to analyze the local ferroelectric switching characteristics[1] and electrical behavior under different magnetic field. Magnetic force microscopy (MFM) in the intermittent contact mode was used to image the magnetic domains and to detect the variation of magnetic domain vibration with external magnetic field.

Plotted in Fig. 1(a) is the XRD collected from the BFO-CFO thin-film nanocomposite. The distinct diffraction peaks are indexed to two sets of peaks, namely the BFO possessing the $R\bar{3}c$ perovskite structure and CFO the spinel structure ($Fd3m$), consistent with previously reported results.[17] No impurity or secondary phase was detected. The out-of-plane lattice parameters for the BFO and CFO components obtained from the XRD are 0.413 nm and 0.803 nm, respectively, corresponding to BFO(001) and CFO(004). These values indicate that BFO is under tensile strain and CFO is compressively strained along the c-axis compared with bulk BFO ($c_{BFO} = 0.396$ nm) and CFO ($c_{CFO} = 0.837$ nm).[21] To further investigate the strain state in this nanocomposite, we collected Raman scattering at room temperature (Fig. 1(b)). The spectra for the BFO-CFO nanocomposite exhibit an intense peak near 685 cm^{-1} associated with CFO (A_{1g} mode) and a relatively weak peak near 205 cm^{-1} which is attributed to the A_1 mode of BFO. These peaks are shifted significantly to lower energies relative to expected energies found in bulk material (BFO: 217 cm^{-1} and CFO: 694 cm^{-1}).[17] This indicates that BFO in our nanocomposite is under tensile strain and CFO possesses a compressive strain,[17] in agreement with the XRD results. Shown in Fig. 1(c) are the well-established in-plane and out-of-plane magnetization hysteresis loops measured at room temperature. No magnetic anisotropy in either direction is observed since nanocomposite is polycrystalline and the size of the components is comparable to the film thickness[12] (Fig. 2). The remnant magnetization is ~37 emu/cm^3 and the coercive field is 1 kOe, smaller than the reported value (>2 kOe)[22] and less than the maximum controllable applied field (2 kOe) for our experimental apparatus.

Shown in Fig. 2(a) is a representative topographic height image for the BFO-CFO nanocomposite film in which the BFO nanoparticles appear to be embedded within surrounding pyramidal-like CFO grains, similar to that for CFO grown on $NdGaO_3$(100).[12] The FE properties of the BFO-CFO nanocomposite film is further investigated using PFM (Figs. 2(b) and 2(c)), where a strong piezoelectric response was observed. Local poling was achieved by scanning in contact mode using a conductive tip ($V_{bias} = +9$ V scanned over a $5 \times 5\ \mu m^2$ area, scan rate 0.5 Hz) immediately followed by application of $V_{bias} = -9$ V scanned over a $3 \times 3\ \mu m^2$ area. The change in the phase contrast in the poled area confirms the FE character of the nanocomposite film, and that the plane normal component of FE polarization can be reoriented.

In order to confirm and quantify the strong ME coupling between BFO and CFO in this nanocomposite thin film, we carried out MFM imaging prior to and following poling of a selected area ($V_{bias} = +9$ V), in combination with PFM mapping[9,23] (Fig. 3). Shown in the insets of Fig. 3 are representative same-area subsets of MFM images collected sequentially from the same larger area (originally collected

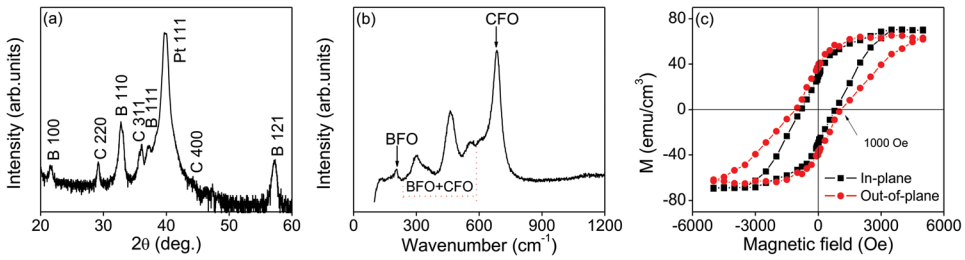

FIG. 1. (a) X-ray diffraction collected from the BFO-CFO nanocomposite thin film. The indexed peaks labeled *B* and *C* correspond to BFO and CFO, respectively; (b) Raman spectrum: arrows denote assigned Raman bands; (c) magnetic hysteresis loops for the in-plane and out-of-plane directions of BFO-CFO nanocomposite thin film measured at 300 K.

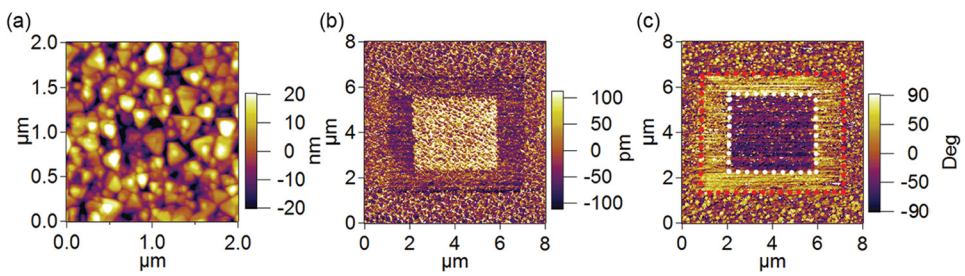

FIG. 2. (a) AFM topographic image ($2 \times 2\ \mu m^2$): results are consistent with BFO nanoparticles embedded within pyramidal CFO nanopillars; (b) and (c) out-of-plane PFM (OP-PFM) amplitude and phase images taken after poling the nanocomposite film using +9 V ($5 \times 5\ \mu m^2$, outside frame) and −9 V ($3 \times 3\ \mu m^2$, inside frame). The poled area is denoted using dashed red lines to convey the change in contrast in both amplitude and phase images in accordance with switched ferroelectric domains.

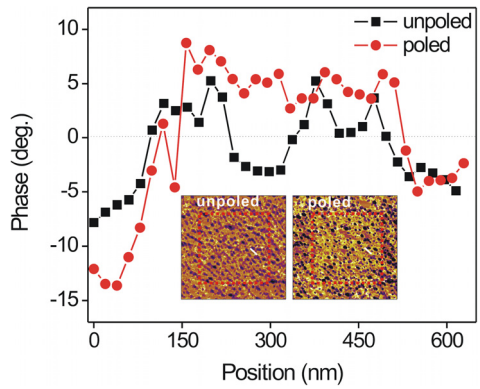

FIG. 3. Line profiles across CFO grains collected from MFM images. The insets are subsets of collected MFM images of the same area ($3 \times 3\ \mu m^2$, red frame) prior to (left) and following (right) electric-field poling, with the white lines denoting the traces from which the line profiles were extracted. The color map corresponds to a range of -5° to $+5^\circ$. These representative results demonstrate that the applied electric field reorients the magnetization of CFO in some areas.

areas were $3 \times 3\ \mu m^2$, 0.5 Hz) for the poled area prior to (left) and following electric field (right) poling, with representative line traces shown in the main part of Fig. 3 corresponding to the white line in each image. Therefore our observation of the reorientation of FM domains within the CFO confirms tuning of the ME coupling via manipulation of the FE polarization orientation in the BFO phase of the nanocomposite thin film.

To further investigate the strain-mediated ME response in the BFO-CFO nanocomposite, we apply an in-plane static magnetic field to the CFO-BFO nanostructure and record the induced variation of PFM amplitude to examine the magnetoelastic coupling under external magnetic field. Interestingly, the obtained amplitude curve versus external magnetic field (Fig. 4(b)) follows the same trend as the measured transverse ME susceptibilities ($\alpha_{31} = \delta E_3/\delta H_1$) as

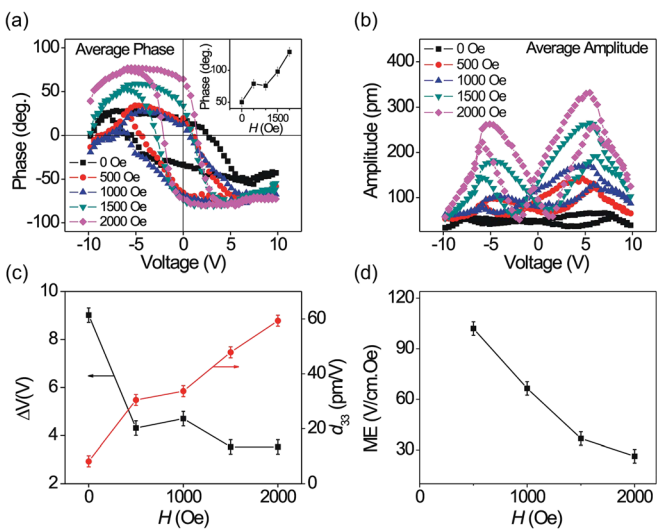

FIG. 4. The local ferroelectric switching characteristics in BFO-CFO nanostructures by the application of external magnetic field by VFM. (a) Average phase-voltage hysteresis loop: the inset shows the remanent phase change as a function of magnetic field; (b) average amplitude-voltage butterfly loop; (c) measured variation in hysteresis loop width and piezoelectric constant d_{33} as obtained from (a) and (b); (d) the ME coefficient as a function of H, calculated from experiment.

that reported in heteroepitaxial BFO-CFO nanostructures, which is the archetypal line of the strain-coupled ME media composed of piezoelectric and magnetostrictive materials.[19,22] The increased amplitude with higher H may be attributed to elongation of the CFO/BFO domains along the in-plane magnetic field.[19] We estimate the transverse magnetoelastic coupling to be $\sim 10 \times 10^{-6}$ according to the amplitude variation (Fig. 4(c)). That the obtained magnetoelastic coupling is much smaller than the reported magnetoelastic coupling in epitaxial BFO-CFO (1–3) structures[9,13,24] ($\sim 350 \times 10^{-6}$) can be attributed to film's polycrystalline (0–3) nature and its lack of magnetic anisotropy.

In-plane application of H resulting in a decrease in the out-of-plane c-axis oriented BFO may be explained by one or both of the following mechanisms. If there is only a BFO layer, an in-plane magnetic field can be expected to cause an in-plane elongation of the lattice. However, since the two lattices are grown in a column-like structure, much stronger magnetic responses from the CFO component cause a large elongation within the plane of the film which, in turn, constrains the BFO in-plane deformation. Due to this stronger in-plane deformation owing to the CFO response, the BFO columns are under compression, leading to an increase in the plane normal c-axis increase and response. A second possibility is that both the BFO and CFO are elongated due the stress induced by the in-plane magnetic field, prior to the application of an electrostatic field across the film. That is, before the electrostatic field is applied, the film is already under a small in-plane stress, producing a very small strain due to the high modulus. The addition of an electrostatic potential on the top of the film can be expected to cause cation displacement, and the existence of an in-plane stress will ease this cation displacement, leading to a larger deformation. The presence of an in-plane stress is confirmed further by our data shown in Fig. 4, in which a coercive field of H_c of $\sim$1 kOe was measured. For a large field ($H > H_c$), a magnetostrictive strain (λ) must be already saturated and the ME coefficient estimated (Fig. 4) should be nearly zero at high field (as a function of piezomagnetic coefficient ($d\lambda/dH$), leading to a maximum in the ME response near H_c. That this is not observed can be taken as further indication of in-plane stresses modifying strain in the structure. The magnetoelastic coupling in CFO should further affect the FE properties of the BFO owing to strong strain-induced polarization rotation.[25,26] Therefore, we collected PFM to detect the local FE switching behavior[28] with applied H. The averaged phase and amplitude loops performed at different values of $|H|$ are shown in Figs. 4(a) and 4(b), respectively.

The phase width changes from $\sim 50^\circ$ to 130° (inset in Fig. 4(a), e.g., -75° to $+75^\circ$ at 2 kOe)), confirming that a trend from incomplete polarization to a near-complete polarization switching process under increasing external magnetic field in the BFO nanocomposite.[1,4,27,29,31,32] The symmetrical characteristic of butterfly loops of the amplitude in Fig. 4(b), altered significantly under applying external magnetic filed, further indicates that the polarization switching process becomes near-complete at high value of H. Here, we can observe that the butterfly loops arrived saturated at about ± 5 V. The hysteresis loops presented in Fig. 4 exhibit an abnormal shape as compared with that typically observed in

pure ferroelectric materials. However, these shapes are similar to those reported in $Pb(Zr,Ti)O_3/CoFe_2O_4$ nanocomposites[11] also exhibiting distinct polarization switching. The butterfly loops of the amplitude in Fig. 4(b) indicate that the piezoelectric amplitude was altered significantly. The coercive voltage, obtained from the overall width of these butterfly loops based on the minima of these loops, is plotted in Fig. 4(c). These values, selected instead of the coercive voltage since there is a small offset of the hysteresis loops along the voltage axis, are seen to decrease for increasing $|H|$, correspond to a reduced domain switching barrier due to the induced magnetostrictive strain. In addition, there is a difference in phase and amplitude response at zero magnetic field and with that for +2 kOe, which can be taken as additional evidence of tuning of ME coupling by manipulation of the FM domains under external magnetic field. In addition, the piezoelectric constant of the nanocomposite can be obtained from the butterfly loops via $d_{33} = A/V_{ac}Q$ where V_{ac} is the applied ac voltage, A is the amplitude, and Q is proportionality factor[30] (Fig. 4(c)). Thus, we determine the lateral ME coefficient[7,27] ($\alpha_{31} = \Delta E_3/\Delta H_1 = \Delta u/Qd_{33}t\Delta H_1$ where ΔE_3 is the change in longitudinal electric field, Δu is the change in piezoresponse amplitude, and t is the thickness of BFO-CFO film ~150 nm) from the amplitude loops at remanent state (Fig. 4(d)). The obtained ME coefficient (the highest value we measure is ~102 mV/cm/Oe) and is comparable to that of bulk PZT-CFO materials (~100 mV/cm/Oe) and other self-assembled epitaxial $BFO_{0.65}$-$CFO_{0.35}$ nanostructures grown on $SrTiO_3$ (from 18 to 120 mV/cm/Oe).[19] Interestingly, the ME coefficient calculated from our measurements is seen to decrease for increasing H. We suggest that the initial tensile strain in the BFO component of the nanocomposite is relaxed for increasing H owing to both ME and magnetostrictive strain coupling; the decreased tensile strain could also result in an increase in the polarization of rhombohedral BFO, as verified by experiment[25] and by first principles calculations.[26] Thus, the evolution of the strain state with H can be indirectly monitored locally during application of an external magnetic field, thereby permitting observation of coupling to ferroelectricity.

In summary, we have shown that a significant ME response can be introduced, and locally probed and manipulated in a BFO-CFO nanocomposite film using an external field in conjunction with a proximal probe, and that quantitative nanoscale ferroelectric switching behavior can be obtained with external magnetic field via PFM. The applied electric field-generated magnetization reversal has been characterized via MFM, enabling quantification of the ME response. We anticipate that these results can motivate further work in the use of local probes for imaging and quantifying ME coupling in multiferroic nano-composite films and related materials.

Work at Drexel supported by the Office of Naval Research. G.C. was supported by the NSF under DMR 0907381.

[1]N. Balke, S. Choudhury, S. Jesse, M. Hujjben, Y. H. Chu, A. P. Baddorf, L. Q. Chen, R. Ramesh, and S. V. Kalinin, Nat. Nanotechnol. **4**, 868 (2009).
[2]S. H. Johnson, P. Finkel, O. D. Leaffer, S. S. Nonnenmann, and J. E. Spanier, Appl. Phys. Lett. **99**, 182901 (2011).
[3]W. Eerenstein, N. D. Mathur, and J. F. Scott, Nature **442**, 759 (2006).
[4]T. Zhao, A. Scholl, F. Zavaliche, K. Lee, M. Barry, A. Doran, M. P. Cruz, Y. H. Chu, C. Ederer, N. A. Spaldin, R. R. Das, D. M. Kim, S. H. Baek, C. B. Eom, and R. Ramesh, Nature Mater. **5**, 823 (2006).
[5]N. Dix, R. Muralidharan, J. M. Rebled, S. Estrade, F. Peiro, M. Varela, J. Fontcuberta, F. Sanchez, and F. Sanchez, ACS Nano **4**, 4955 (2010).
[6]R. Ramesh and N. A. Spaldin, Nature Mater. **6**, 21 (2007).
[7]C. W. Nan, M. I. Bichurin, S. Dong, D. Viehland, and G. Srinivasan, J. Appl. Phys. **103**, 031101 (2008).
[8]H. Zheng, J. Wang, S. E. Lofland, Z. Ma, L. Mohaddes-Ardabili, T. Zhao, L. Salamanca-Riba, S. R. Shinde, S. B. Ogale, F. Bai, D. Viehland, Y. Jia, D. G. Schlom, M. Wuttig, A. Roytburd, and R. Ramesh, Science **303**, 661 (2004).
[9]F. Zavaliche, T. Zhao, H. Zheng, F. Straub, M. P. Cruz, P. L. Yang, D. Hao, and R. Ramesh, Nano Lett. **7**, 1586 (2007).
[10]H. Luo, H. Yang, S. A. Baily, O. Ugurlu, M. Jain, M. E. Hawley, T. M. McCleskey, A. K. Burrell, E. Bauer, L. Civale, T. G. Holesinger, and Q. Jia, J. Am. Chem. Soc. **129**, 14132 (2007).
[11]X. Gao, B. J. Rodriguez, L. Liu, B. Birajdar, D. Pantel, M. Ziese, M. Alexe, and D. Hesse, ACS Nano **4**, 1099 (2010).
[12]S. C. Liao, P. Y. Tsai, C. W. Liang, H. J. Liu, J. C. Yang, S. J. Lin, C. H. Lai, and Y. H. Chu, ACS Nano **5**, 4118 (2011).
[13]Z. Wang, Y. Yang, R. Viswan, J. Li, and D. Viehland, Appl. Phys. Lett. **99**, 043110 (2011).
[14]I. Stern, J. He, X. Zhou, P. Silwal, L. Miao, J. M. Vargas, L. Spinu, and D. H. Kim, Appl. Phys. Lett. **99**, 082908 (2011).
[15]I. Levin, J. Li, J. Slutsker, and A. L. Roytburd, Adv. Mater. **18**, 2044 (2006).
[16]H. Zheng, F. Straub, Q. Zhan, P. L. Yang, W. K. Hsieh, F. Zavaliche, Y. H. Chu, U. Dahmen, and R. Ramesh, Adv. Mater. **18**, 2747 (2006).
[17]O. Chaix-Pluchery, C. Cochard, P. Jadhav, J. Kreisel, N. Dix, F. Sanchez, and J. Fontcuberta, Appl. Phys. Lett. **99**, 072901 (2011).
[18]N. Dix, R. Muralidharan, J. Guyonnet, B. Warot-Fonrose, M. Varela, P. Paruch, F. Sanchez, and J. Fontcuberta, Appl. Phys. Lett. **95**, 062907 (2009).
[19]Y. S. Oh, S. Crane, H. Zheng, Y. H. Chu, R. Ramesh, and K. H. Kim, Appl. Phys. Lett. **97**, 052902 (2010).
[20]F. Yan, M. O. Lai, L. Lu, and T. J. Zhu, J. Phys. Chem. C **114**, 6994 (2010).
[21]F. Yan, T. J. Zhu, M. O. Lai, and L. Lu, Appl. Phys. Express **4**, 111502 (2011).
[22]L. Yan, Z. Xing, Z. Wang, T. Wang, G. Lei, J. Li, and D. Viehland, Appl. Phys. Lett. **94**, 192902 (2009).
[23]F. Zavaliche, H. Zheng, L. Mohaddes-Ardabili, S. Y. Yang, Q. Zhang, P. Shafer, E. Reilly, R. Chopdekar, Y. Jia, P. Wright, D. G. Schlom, Y. Suzuki, and R. Ramesh, Nano Lett. **5**, 1793 (2005).
[24]R. M. Bozorth, E. F. Tilden, and A. J. Wiliams, Phys. Rev. **99**, 1788 (1955).
[25]H. W. Jiang, S. H. Baek, D. Ortiz, C. M. Folkman, R. R. Das, Y. H. Chu, P. Shafer, J. X. Zhang, S. Choudhury, V. Vaithyanathan, Y. B. Chen, D. A. Felker, M. D. Biegalski, M. S. Rzchowski, X. Q. Pan, D. G. Schlom, L. Q. Chen, R. Ramesh, and C. B. Eom, Phys. Rev. Lett. **101**, 107602 (2008).
[26]C. Ederer and N. A. Spaldin, Phys. Rev. Lett. **95**, 257601 (2005).
[27]S. Xie, F. Ma, Y. Liu, and J. Li, Nanoscale **3**, 3152 (2011).
[28]D. Mazumdar, V. Shelke, M. Iliev, S. Jesse, A. Kumar, S. V. Kalinin, A. P. Baddorf, and A. Gupta, Nano Lett. **10**, 2555 (2010).
[29]G. Catalan and J. F. Scott, Adv. Mater. **21**, 2463 (2009).
[30]A. Yourdkhani, A. K. Perez, C. Lin, and G. Caruntu, Chem. Mater. **22**, 6075 (2010).
[31]R. Proksch and S. V. Kalinin, Microbiol. Today **17**, 10 (2009).
[32]A. N. Morozovska, E. A. Eliseev, N. Balke, and S. V. Kalinin, J. Appl. Phys. **108**, 053712 (2010).